ISSN 1330-3651 (Print), ISSN 1848-6339 (Online)
Received: 17 April 2025; Accepted: 24 August 2025

https://doi.org/10.17559/TV-20250417002603
Original scientific paper

Advancements in Photogrammetric Modelling: Boundary Marking for Improved Accuracy

Hasan Kemal SURMEN

Abstract: Photogrammetric modelling, a widely used technique for reconstructing 3D models from photographic data, relies on achieving high geometric accuracy to minimize post-processing efforts. This study proposes an enhancement to the photogrammetric reconstruction workflow through the introduction of the Boundary Marking Technique. By visibly marking the edges surrounding object surfaces, this method aims to improve edge definition and overall reconstruction quality. The technique was applied to both metal and plastic objects of identical geometry. 3D models were generated using close-range photogrammetry for both marked and unmarked versions, and deviation analyses were conducted against their CAD references. A total of 16 analyses comprising one 3D and three 2D per object were performed using computer-aided comparison tools. Results indicate that the Boundary Marking Technique significantly enhances geometric accuracy, particularly along edges and adjacent surfaces, ultimately improving model topology and dimensional fidelity across the entire reconstruction.

Keywords: 3D reconstruction; boundary marking; CAD; geometric accuracy; photogrammetry; reverse engineering

1 INTRODUCTION

Today, 3D reconstruction methods are widely used to create 3D models of objects or scenes for various applications, including reverse engineering [1], metrology analysis [2], 3D printing [3, 4], and computer-aided engineering (CAE) simulations [5-7]. One of these techniques is photogrammetry, an image-based modelling method [8]. Photogrammetry is utilized in diverse fields, including archaeology [9], architecture [10], historical and cultural heritage [11], biomedical [12], medical [13], forensic [14], augmented reality/virtual reality (AR/VR) [15], gaming [16], and engineering applications [17, 18].

Close-range photogrammetry is a technique employed to generate 3D models of objects. In this method, digital 3D geometric data of an object is acquired by capturing multiple overlapping photographs from various angles. This data is then processed using specialized software to create the 3D model. While photogrammetry offers advantages such as low cost, portability, wide scanning range, and photorealistic texture, it has certain limitations in terms of geometric accuracy, especially when compared to advanced 3D scanning technologies, as it relies solely on photographic data [19]. As a result, enhancing geometric accuracy and developing new methodologies are crucial in the field of photogrammetry [20, 21].

Several factors during the photography stage can negatively impact photogrammetric modelling. These factors can be attributed to the operator, the environment, and the object itself. The geometry, material, and texture of the object's surface and edges are critical factors affecting reconstruction quality. For instance, glossy materials, rough surfaces, and polished finishes can reduce geometric accuracy and introduce defects in the 3D models. Additionally, shadows on the object can negatively influence photogrammetry. Shadows may result from the environment or specific object features, such as ribs. Blank textures can obscure transitions between different surfaces, and rounded concave edges may cause visual blurring. In photogrammetry, the RGB (red, green, blue) colour data of the object is captured from photographs. Segmentation is a fundamental process for processing point cloud data and reconstructing scanned objects [22]. Photogrammetry software, such as Autodesk-ReCap Photo, Agisoft-Metashape, and AliceVisionMeshroom [23-25], can assign RGB values from captured images to the points and polygons of the 3D model. However, the challenge arises when different object features share similar colours, which can prevent effective colour segmentation and hinder reconstruction accuracy. These factors contribute to the limitations of photogrammetry, especially regarding geometric precision.

Post-processing mesh repair operations are commonly used to correct geometric defects in the 3D model after digitization. The success of these repair operations varies depending on the effort and expertise involved. In some cases, surface defects may be beyond repair. Various techniques, such as marking [1, 26], coating [27-29], and masking [30], are employed to enhance the geometric accuracy of 3D models. These methods may require significant time and skilled personnel, both before and after scanning.

This study introduces the boundary marking technique (BMT) as a pre-photogrammetry preparation step to improve the quality of 3D reconstructions by making the surface boundaries of objects more distinguishable during photogrammetric digitization. The technique has been thoroughly investigated, and its impact on geometric accuracy has been demonstrated through 3D and 2D deviation analysis. Notably, the BMT requires no additional resources and facilitates efficient object preparation for 3D scanning within a short time frame.

The effectiveness of this innovative technique in enhancing geometric accuracy was investigated using a machine part with ribs and concave edges. To observe the effects of the technique more clearly, the object was CNC-machined from a single-coloured, uniform, and smooth-textured metal and plastic material, ensuring consistent dimensions. Close-range photogrammetry was employed as the 3D digitization method. No auxiliary systems, such as laser or projection, or methods like coating or masking were used that could influence the modelling process. The photography phase was performed under the same conditions for each model. After obtaining the 3D models of metal and plastic sample objects using photogrammetry, the models were reconstructed again after marking the edges. A CAD model, created based on the physical object's dimensions, was used as a reference for comparing

the 3D models generated from the marked and unmarked objects. Geometric accuracy was analysed using both 3D and 2D comparison methods, utilizing 3D Systems Geomagic Control X software. The improvement in geometric accuracy through the application of the boundary marking technique is detailed through both 3D body and various 2D section analyses of the metal and plastic objects. The results from four objects were compared with the reference CAD model, and these findings were then cross-analysed.

2 METHOD

There are two main types of photogrammetry: terrestrial and aerial. Terrestrial photogrammetry, also referred to as close-range photogrammetry, is typically used for distances up to 200 meters [31]. The close-range photogrammetry method employed in this study is specifically designed for digitizing small-scale 3D objects, rather than for generating topographic maps. This technique is also known as 3D photogrammetry [32] or image-based 3D modelling [33] when used to produce three-dimensional reconstruction of objects.

The fundamental principle of photogrammetry is triangulation, which enables the calculation of 3D point coordinates. A point's spatial position is determined by mathematically intersecting lines of sight from multiple camera angles. In practice, at least two photographs taken from different perspectives are used to establish lines of sight from the camera to the target point. The intersection of these lines yields the *X*, *Y*, and *Z* coordinates of the point, based on the known camera positions and orientations. Once the 3D point data are obtained, a point cloud model of the object can be generated using specialized software. This point cloud can then be transformed into a polygonal mesh model [34].

Photogrammetry offers the advantage of producing 3D models with photorealistic textures, as it captures both geometric and texture information - unlike other 3D scanning methods such as laser scanning or CT scanning. It is also portable and cost-effective, requiring no electrical connections, and supports a wide range of scales, from small objects to large structures. For these reasons, photogrammetry is widely adopted across various disciplines. However, despite its advantages, photogrammetry can be limited in terms of geometric accuracy. To address this, the present study employs photogrammetry as the 3D digitization method and introduces the boundary marking technique to enhance geometric precision.

The workflow of this research is illustrated in Fig.1, which includes object preparation, image acquisition, 3D reconstruction, geometric accuracy evaluation, and comparative analysis of the results.

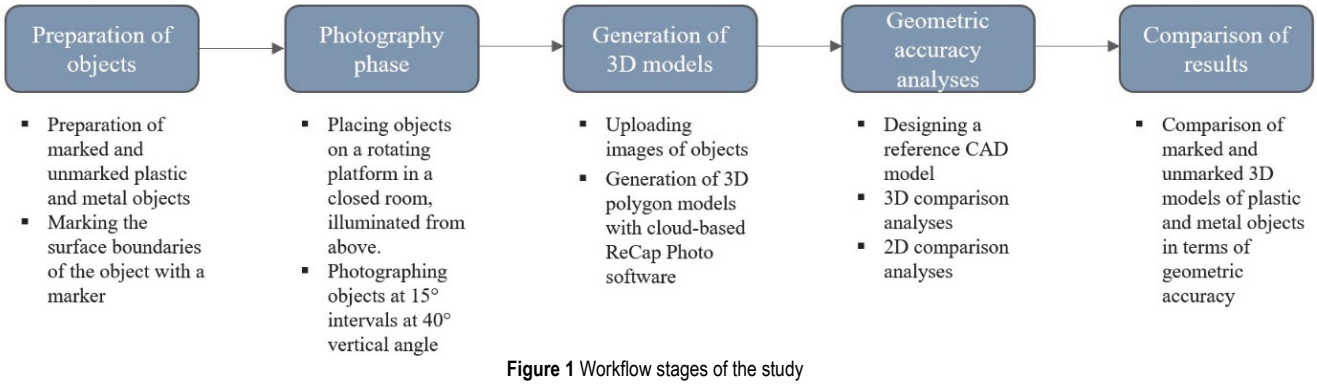

Figure 1 Workflow stages of the study

2.1 Preparation of Sample Objects and Generation of 3D Models by Photogrammetry

The sample objects were manufactured in the same dimensions from metal and plastic materials by the CNC method. The marked objects were obtained by drawing the boundaries of plastic and metal objects with an erasable marker pen and prepared for photogrammetric modelling (Fig. 2). Manual marking was implemented due to the complex and varying geometries of the objects, which limit the feasibility of automated methods. To ensure consistency, all markings were performed by the same operator using a marker with a line width generally between 0.5 mm and 2 mm. This range was found to be optima - thin enough to preserve geometric detail, yet thick enough to ensure reliable detection in the images. In certain cases, especially under along concave edges, slightly thicker lines were used to enhance visibility.

3D models of marked and unmarked objects were created by photogrammetry using cloud-based Autodesk-ReCap Photo software. 24 photographs of each object were taken at 15-degree intervals. The camera was fixed at a vertical angle of 37 degrees during photography. There is an 80-90% overlap between images. Canon EOS 50D camera and 18-135 mm lens were used for photography.

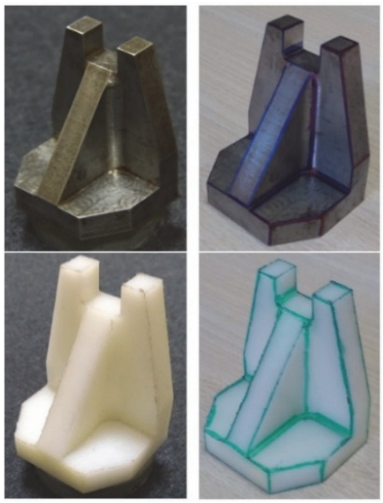

Figure 2 Unmarked and marked metal and plastic objects used for photogrammetric modelling

Photography was performed in an indoor environment. A rotating platform was used to avoid operator error and to achieve the same photo overlap rate (Fig.3). A blank fabric that does not reflect light was used for the floor and background. The same workflow was implemented for the photogrammetric modelling of all objects. After the 3D models were generated, the ground part outside the object model was removed in the ReCap Photo software. No editing was done on the 3D models. The objects generated with the RCM (Reality Capture Mesh) format were exported in OBJ (WaveFrontOBJect) format for 3D and 2D deviation analyses.

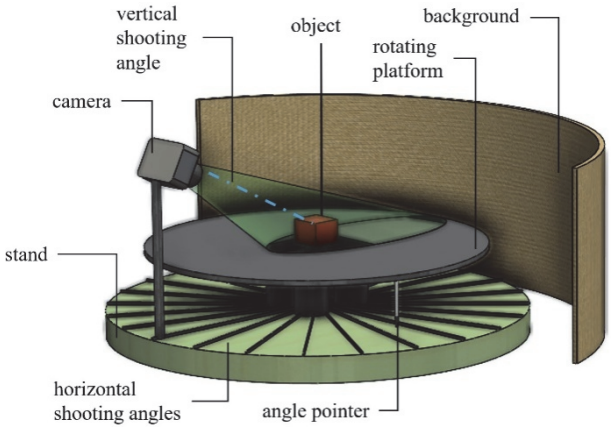

Figure 3 Setup for photography

2.1 Comparison of Reconstructed Models

Computer-aided engineering software specialized in the field of 3D scanning is used to analyse the accuracy of scanned data and for measurement and alignment applications [35].

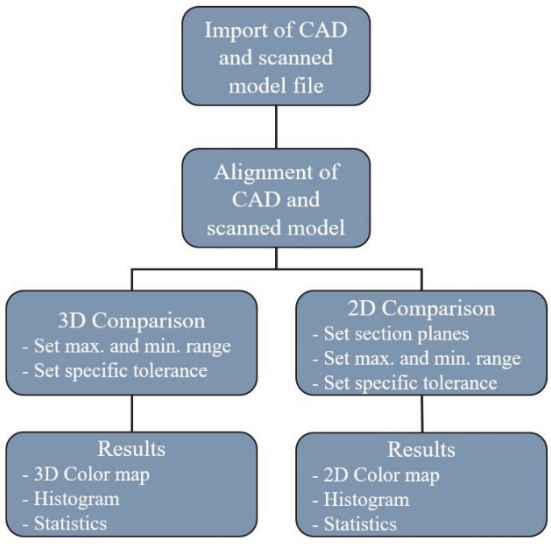

Figure 4 Workflow for comparing of each model generated from marked and unmarked metal and plastic objects

To see the effects of the boundary marking technique on 3D reconstruction in detail, marked and unmarked 3D models of plastic and metal objects were compared for geometric accuracy using Geomagic Control X software. A reference CAD model was used for these comparisons. The CAD model was drawn using CAD software according to the dimensions of the CNC machined parts. The bounding box dimensions of the model are 60 × 50 × 40 mm. The four reconstructed 3D models and the CAD model were separately compared for geometric accuracy and analysed between the reference and scanned data. 3D and 2D comparison methods were used for the analyses. The workflow shown in Fig. 4 was followed for the comparison of each generated model.

In the 3D comparison analysis, the 3D geometric data of the reconstructed models were compared with the reference data derived from the CAD model and the deviations were measured. As for the 2D comparisons, three different 2D sections were determined. These section planes were created especially considering the edges and corners of the object, which are critical for scanning. In the 2D comparison analyses, the reconstructed models and the CAD model were compared with reference to these section planes. The tolerance value for all comparisons was set to 0.5 mm. A total of 16 comparison analyses were performed, one 3D and three 2D analyses for four scanned model.

The total number of points is called n in the 3D compare and each measured vertex is defined by a Measured Position (P_m) and a Reference Position (P_r).

$$P_m = (x_m, y_m, z_m) \tag{1}$$

$$P_r = (x_r, y_r, z_r) \tag{2}$$

A Gap Vector (GV) is calculated for each measured point. GV goes from the P_r to P_m.

$$GV = (x_m - x_r, y_m - y_r, z_m - z_r) \tag{3}$$

GV is converted to a scalar magnitude and it is called the Gap Distance (D). D is the deviation value at any given point. If the measured point is on the negative side of the reference data D is given a negative value. Deviation can be used instead of Gap Distance.

$$D = \sqrt{GV_x^2 + GV_y^2 + GV_z^2} \tag{4}$$

The explanation of the statistics obtained as a result of the analyses is given below: Max: It is the largest positive deviation. Min: It is the largest negative deviation. Average (A): The arithmetic mean of all the deviations.

$$A = \frac{1}{n}\sum_{i=1}^{n} D_i \tag{5}$$

RMS: *RMS* (Root Mean Square) is a measure of the magnitude of all deviation values.

$$RMS = \sqrt{\frac{1}{n}\sum_{i=1}^{n} D_i^2} \tag{6}$$

Std. Dev.: It is the standard deviation of all the gap distance values.

$$\sigma = \sqrt{\frac{1}{n}\sum_{i=1}^{n}(D_i - A)^2} \quad (7)$$

Var.: It is the variance of the deviations.

$$Var = \sigma^2 \quad (8)$$

+Avg: It is the mean of all the positive deviations. −Avg: It is the mean of all the negative deviations. In Tol. (%): It is the percentage of points within the defined tolerance. Out Tol. (%): It is the percentage of points outside of the defined tolerance. Over Tol. (%): It is the percentage of points that are greater than the upper tolerance limit. Under Tol. (%): It is the percentage of points that are less than the upper tolerance limit.

3 RESULTS

The 3D models were generated using the close-range photogrammetry method. Solid, mesh, and textured views of the 3D models, both for the unmarked and marked metal and plastic objects, are presented in Figs. 5 and 6.

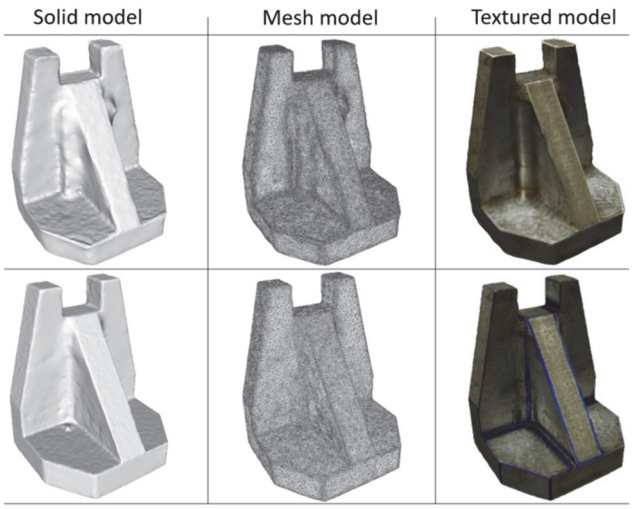

Figure 5 Solid, mesh and textured models generated from the metal object before (first row) and after (second row) the application of BMT

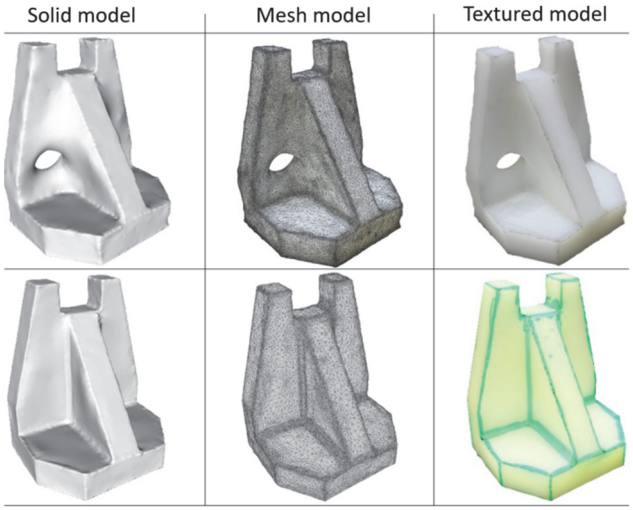

Figure 6 Solid, mesh and textured models generated from the plastic object before (first row) and after (second row) the application of BMT

The edges of the model generated from the marked object were reconstructed with greater accuracy and sharpness. The geometric defects along the concave edges on both sides of the rib, which were apparent in the unmarked models, were significantly reduced through the application of the boundary marking technique. Furthermore, the hole defect observed in the unmarked plastic model was completely eliminated after marking. Improvements were also observed in the accuracy of the outer edges. These enhancements in edge clarity contributed positively to the overall geometric accuracy of the model surfaces.

3.1 Results of 3D Deviation Analyses

The deviation between the measured and reference data was analysed by projecting all paired points onto the reference data using the "3D Compare" tool in Geomagic Control X software. The deviation is displayed with a colour map that helps analyse positive and negative deviation plots through the entire part.

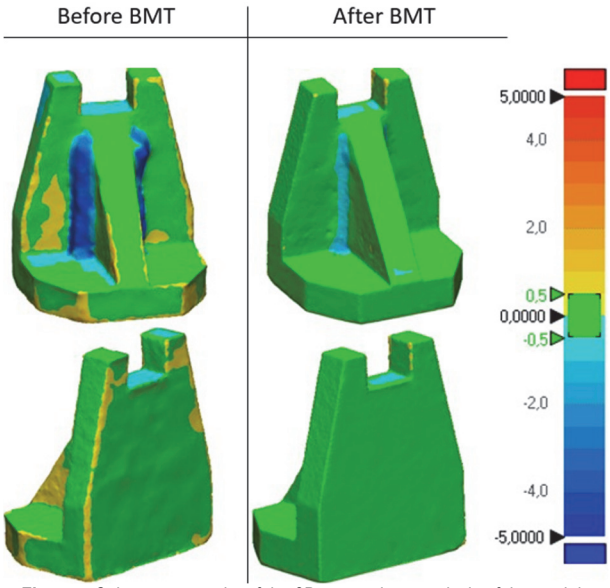

Figure 7 Colour map results of the 3D comparison analysis of the models generated from the metal object before and after the application of BMT

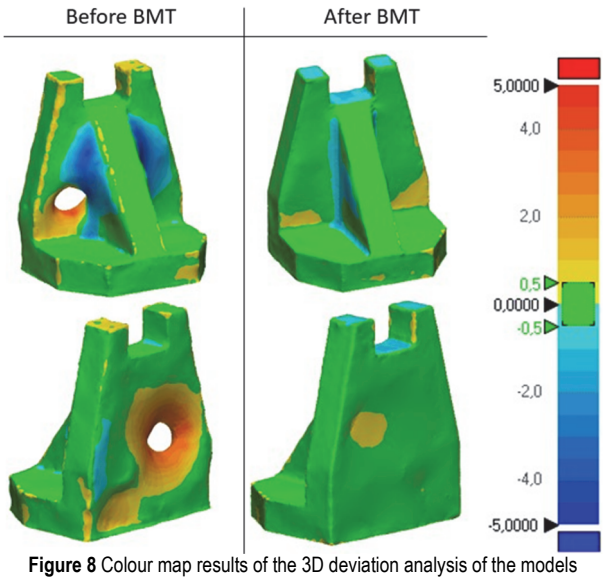

Figure 8 Colour map results of the 3D deviation analysis of the models generated from the plastic object before and after the application of BMT

3D models (measured data) generated from unmarked and marked metal and plastic objects were compared to a CAD model (reference data) drawn according to the actual dimensions of the object to better observe the usefulness of the boundary marking technique. The colour map and histogram results are shown in Figs. 7 to 10 and the statistical results are shown in Tabs. 1 and 2 for the results of the deviation (comparison) analyses.

The 3D deviation analysis colour map results obtained by comparing the photogrammetric models with the CAD model are shown in Fig. 7 (for the metal object) and Fig. 8 (for the plastic object). The green colour shows the regions within the tolerance range of ±0.5mm in the colour map. As the deviation increases in a negative direction, the colour changes to dark blue; as the deviation increases in a positive direction, it changes to red. Blue is seen on the concave edges and yellow and orange on the outer edges of the unmarked metal model. It is seen that the green area in the colour map of the marked model increases compared to the unmarked model and the size of the deviations decreases. Also, the green areas increased and the high deviation values decreased compared to the unmarked model on the marked plastic model. Similar improvements were observed in geometric accuracy with the boundary marking technique in both comparisons.

The statistical data obtained as a result of the 3D deviation analyses are shown in detail in Tab. 1 for the models generated from the metal object and in Tab. 2 for the models generated from the plastic object before and after the application of BTM. These values were compared for the marked and unmarked objects, and the improvements in geometric accuracy obtained are shown as percentages in Tab. 3.

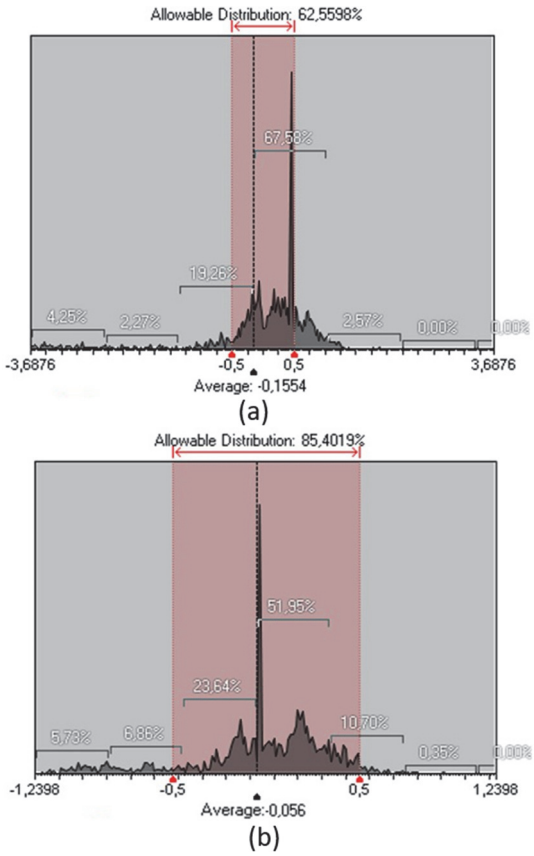

Figure 9 Histogram results of the 3D comparison analysis of the models generated from the metal object: (a) before, (b) after the application of BMT

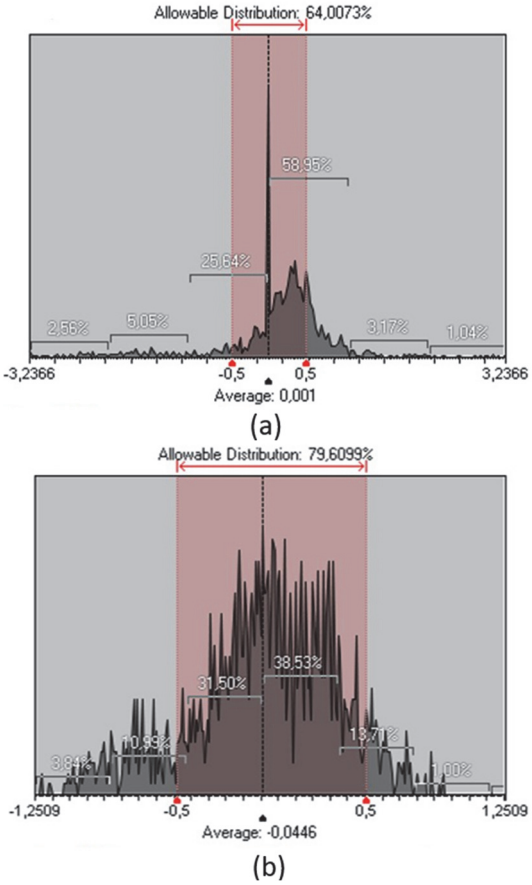

Figure 10 Histogram results of the 3D comparison analysis of the models generated from the plastic object: (a) before, (b) after the application of BMT

Table 1 Statistical results of the 3D comparison analysis of the models generated from the metal object before and after the application of BMT

Statistical Parameters	Models generated from the metal object	
	Before BMT	After BMT
Min.	−4,4102	−2,1807
Max.	1,8797	1,077
Avg.	−0,1554	−0,056
RMS	1,1876	0,3986
Std. Dev.	1.1774	0,3946
Var.	1,3862	0,1557
+Avg.	0,4675	0,2313
−Avg.	−1,0664	−0,3192
In Tol. (%)	62.5598	85,4019
Out Tol. (%)	37.4402	14,5981
Over Tol. (%)	20,9928	2,2459
Under Tol. (%)	16,4474	12,3522

Table 2 Statistical results of the 3D comparison analysis of the models generated from the plastic object before and after the application of BMT.

Statistical Parameters	Models generated from the plastic object	
	Before BMT	After BMT
Min.	−4,4322	−1,4287
Max.	4,3223	0,9209
Avg.	0,001	−0,0446
RMS	1,0785	0,4046
Std. Dev.	1,0785	0,4021
Var.	1,1633	0,1617
+Avg.	0,5096	0,2758
−Avg.	−0,8918	−0,346
In Tol. (%)	64,0073	79,6099
Out Tol. (%)	35,9927	20,3901
Over Tol. (%)	21,1937	7,2695
Under Tol. (%)	14,799	13,1206

BMT reduced the minimum deviation for the metal model by 51% and the maximum deviation by 43%. The standard deviation decreased by 66%. The region within

tolerance increased by 37%. The region out of tolerance decreased by 61%.

The hole defect observed in the unmarked plastic model was completely eliminated following the application of the marking technique. As a result of this improvement, the minimum deviation decreased by 68%, the maximum deviation by 79%, and the standard deviation by 63%. The area within the acceptable tolerance range increased by 24%, while the area outside the tolerance range decreased by 43%.

Table 3 Improvement of the geometric accuracy by means of the boundary marking technique on the basis of the 3D comparison analyses.

Statistic Parameters	Improvement in metal model / %	Improvement in plastic model / %
Min.	51	68
Max.	43	79
RMS	66	62
Std. Dev.	66	63
Var.	89	86
+Avg.	51	46
−Avg.	70	61
In Tol. (%)	37	24
Out Tol. (%)	61	43
Over Tol. (%)	89	66
Under Tol. (%)	25	11

3.2 Results of 2D Deviation Analyses

To better observe the improvements in surface quality and edge accuracy, 2D deviation analyses were conducted for both metal and plastic models, using the CAD model as a reference. The "2D Compare" tool evaluates the deviation between the measured data and the reference model on specific section planes, providing a 2D sectional view of the analysed region. The reconstructed models were compared with the CAD model across three sectional planes, defined based on their offset distances from the base plane of the 3D models. The locations of these section planes and the corresponding 2D analysis results are illustrated on the 3D models in Fig. 11.

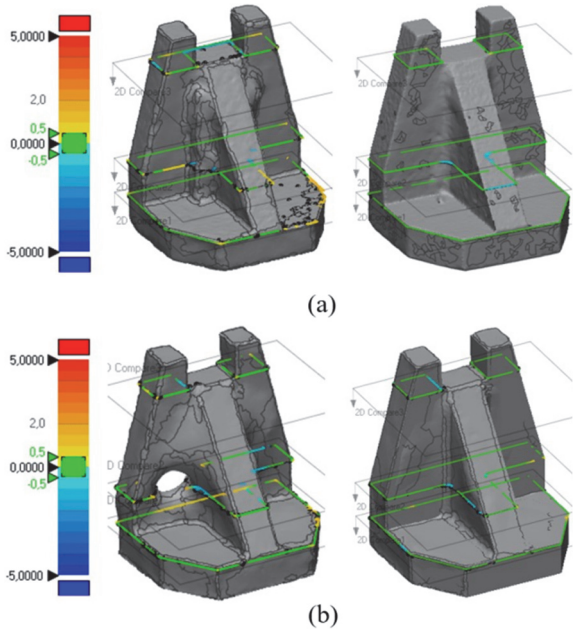

Figure 11 Demonstration of 2D comparison results obtained according to three different section planes on the 3D models: (a) the models generated from the metal object before and after the application of BMT, (b) the models generated from the plastic object before and after the application of BMT

Detailed colour map results before and after the application of the Boundary Marking Technique (BMT) are presented in Fig. 12 for the metal object and in Fig. 13 for the plastic object. Statistical analysis results before and after BMT application are summarized in Tab. 4 for the metal object and in Tab. 5 for the plastic object.

The boundary marking technique enhanced the geometric accuracy across all 2D section planes reconstructed from both plastic and metal objects. As shown in Figs. 12 and 13, the regions falling within the tolerance range of ±0.5 mm have increased, indicating improved cross-sectional geometries. Geometric deviations for both unmarked and marked models in each section plane are illustrated using a whisker plot. The colour scheme in the whisker representation corresponds to that of the colour map. It is evident that the green regions - representing areas within the acceptable deviation range - are more prominent in all section planes of the model derived from the marked object, while the magnitude of deviations has decreased overall.

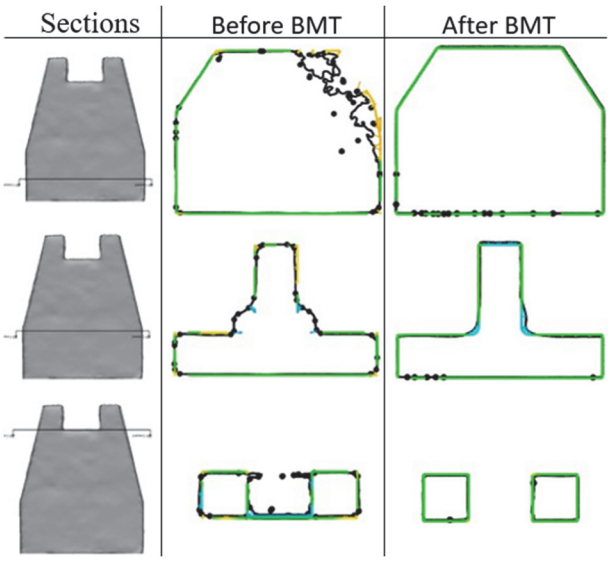

Figure 12 Results of the 2D comparison analysis of the models generated from the metal object before and after the application of BMT with respect to three section planes

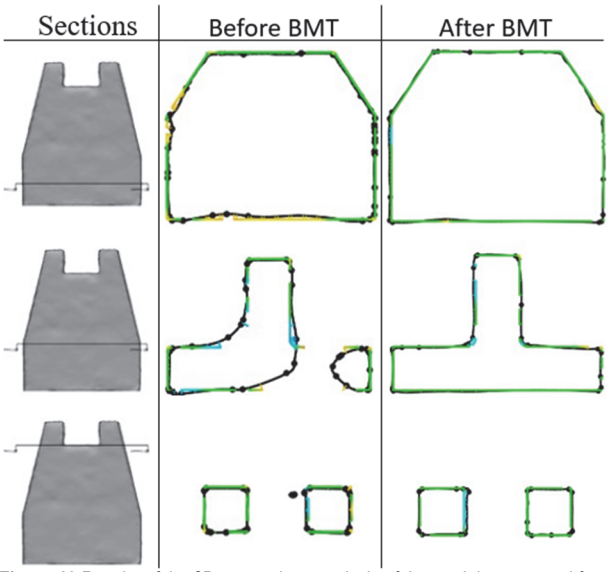

Figure 13 Results of the 2D comparison analysis of the models generated from the plastic object before and after the application of BMT with respect to three section planes

The statistical results obtained before and after the application of the Boundary Marking Technique (BMT) also provide numerical evidence that the technique enhances photogrammetric modelling. For the metal object (Tab. 4), a 69% improvement was observed in Section 1, with the standard deviation decreasing from 0.54 to 0.17. The region within the tolerance range increased from 70% to 100%, corresponding to a 43% improvement compared to the unmarked model. In Section 2, a 30% improvement was achieved by reducing the standard deviation from 0.65 to 0.45, while the region within tolerance increased from 68% to 76%, reflecting an 11% improvement. In Section 3, the standard deviation decreased from 0.47 to 0.20, indicating a 57% improvement. The region within tolerance increased from 67% to 97%, corresponding to a 44% improvement over the unmarked model.

For the plastic object (Tab. 5), the application of the Boundary marking technique also led to significant improvements. In Section 1, a 21% improvement was achieved by reducing the standard deviation from 0.33 to 0.26. The region within the tolerance range increased from 73% to 94%, corresponding to a 29% improvement compared to the unmarked model. In Section 2, the standard deviation decreased from 0.80 to 0.37, indicating a 54% improvement. The region within tolerance increased from 62% to 81%, showing a 31% improvement. In Section 3, the standard deviation was reduced from 0.37 to 0.29, representing a 20% improvement. The region within tolerance increased from 78% to 91%, which corresponds to a 16% improvement compared to the unmarked model.

Table 4 Statistical results of the 2D comparison analysis of the models generated from the metal object before and after the application of BMT with respect to three section planes

Statistic Parameters	Section 1		Section 2		Section 3	
	Before BMT	After BMT	Before BMT	After BMT	Before BMT	After BMT
Min.	−0,2077	−0,3587	−2,0376	−1,0787	−1,675	−0,1789
Max.	1,9719	0,3139	1,1952	0,4724	0,8093	0,5773
Avg.	0,3888	−0,0984	0,1344	−0,0781	0,066	0,1652
RMS	0,6636	0,1939	0,6631	0,4588	0,4759	0,2611
Std. Dev.	0,5377	0,167	0,6493	0,4521	0,4713	0,2022
Var.	0,2892	0,0279	0,4216	0,2044	0,2221	0,0409
+Avg.	0,5687	0,0955	0,4356	0,2304	0,409	0,2689
−Avg.	−0,0942	−0,1933	−0,5775	−0,5205	−0,404	−0,1458
In Tol.(%)	69,7674	100	68,4685	75,969	67,1875	96,875
Out Tol.(%)	30,2326	0	31,5315	24,031	32,8125	3,125
Over Tol.(%)	30,2326	0	21,6216	0	18,75	3,125
Under Tol.(%)	0	0	9,9099	24,031	14,0625	0

Table 5 Statistical results of the 2D comparison analysis of the models generated from the plastic object before and after the application of BMT with respect to three section planes

Statistic Parameters	Section 1		Section 2		Section 3	
	Before BMT	After BMT	Before BMT	After BMT	Before BMT	After BMT
Min.	−0,433	−0,5536	−1,5731	−0,9867	−0,9843	−0,9366
Max.	1,2458	0,6859	2,103	0,8184	1,1239	0,3915
Avg.	0,3638	−0,0223	−0,0602	−0,1475	0,1799	−0,0268
RMS	0,4931	0,2627	0,7998	0,3983	0,409	0,2959
Std. Dev.	0,3329	0,2618	0,7975	0,3699	0,3674	0,2947
Var.	0,1108	0,0685	0,6361	0,1369	0,135	0,0868
+Avg.	0,4049	0,1927	0,5499	0,2278	0,3485	0,176
−Avg.	−0,2996	−0,2163	−0,6819	−0,3914	−0,2962	−0,3431
In Tol. (%)	72,9927	94,1606	61,6822	81,0606	78,4615	90,625
Out Tol. (%)	27,0073	5,8394	38,3178	18,9394	21,5385	9,375
Over Tol. (%)	27,0073	2,9197	12,1495	3,7879	13,8462	0
Under Tol. (%)	0	2,9197	26,1682	15,1515	7,6923	9,375

4 DISCUSSION

Photogrammetry is an image-based modelling technique that offers advantages such as low cost, photorealistic texture, and portability. However, its reliance solely on photographic data limits its ability to accurately reconstruct objects with smooth surfaces or monochromatic, textureless regions, often resulting in lower geometric accuracy. Enhancing geometric accuracy is therefore critical in photogrammetric modelling, and many studies have explored this issue by comparing photogrammetric models with those obtained using alternative 3D scanning technologies [23, 36-40]. Beyond software-based improvements, surface coating techniques have also been investigated to enhance accuracy [41, 42].

This study introduced and evaluated the boundary marking technique, which aims to improve surface segmentation and, consequently, model accuracy. For the first time, the technique was assessed using detailed quantitative data by comparing photogrammetric reconstructions of both marked and unmarked plastic and metal objects with a CAD reference model. This model, created based on precise real-world dimensions, enabled an accurate evaluation of photogrammetric reconstructions using engineering software.

The results demonstrated a significant improvement in geometric accuracy when the technique was applied. The boundary marking technique positively affected dimensional accuracy, improved surface topology, and reduced geometric defects. This is particularly important for objects with complex features - such as the test object used in this study, which included surfaces in 11 directions, channels, ribs, concave corners, and smooth,

monochromatic textures in both plastic and metal materials.

Previous research has shown that photogrammetric reconstructions often struggle to segment featureless or low-contrast surfaces, resulting in blurred or merged boundaries [43, 44]. This study addresses this limitation by proposing a non-invasive and easily applicable method for enhancing boundary definition.

In image-based modelling, similar or textureless surfaces often lead to errors in surface segmentation and reconstruction. As noted in image processing literature, segmentation is a major challenge [45]. Drawing along object boundaries with a marker helps distinguish adjacent surfaces, making the segmentation process more reliable.

Quantitative results from 3D comparison analyses showed that for metal objects, the boundary marking technique led to a 43% improvement in maximum deviation and a 51% improvement in minimum deviation within ±0.5 mm tolerance. For plastic objects, improvements were even more notable: 79% (max.) and 68% (min.) respectively. The proportion of surface area within tolerance increased by 37% in the metal object and 24% in the plastic one. Moreover, structural features such as bone-like elements and holes that were lost in the unmarked models were accurately reconstructed when the technique was used.

In contrast to coating or speckle pattern application methods - which can be time-consuming, expensive, or leave residues - the boundary marking technique offers a reversible, low-cost solution. Comparable approaches, such as the use of projected patterns (e.g., structured light or coded targets), have shown improvements in accuracy [46], but these require additional hardware. In this context, the proposed method achieves similar gains without extra instrumentation, offering practicality for field applications or rapid digitization scenarios.

The 2D comparison analysis further supported the 3D findings. Three planar sections were defined and evaluated in both marked and unmarked models. After applying the technique, the regions within ±0.5 mm tolerance increased substantially: 43%, 11%, and 44% for the metal object across the three planes; and 29%, 32%, and 16% for the plastic object, respectively.

These findings reinforce the practical value of the boundary marking technique, particularly in application areas such as reverse engineering, where reconstruction accuracy is critical.

Compared to previous surface enhancement methods in photogrammetry - such as speckle pattern application, surface coating, or active projection systems - the proposed boundary marking technique stands out due to its simplicity, reversibility, and minimal resource requirements.

While methods like structured light scanning or powder spraying have shown high accuracy [43, 46], they may not be suitable for delicate or real-world field objects. In contrast, the boundary marking technique requires no permanent surface alteration or additional equipment, offering a practical and adaptable solution. This distinction underlines the novel contribution of this study and opens up new opportunities for low-cost, accurate digitization workflows.

5 CONCLUSION

The boundary marking technique proposed to improve geometric accuracy in 3D reconstruction applications was investigated in this study. In this method, the boundaries of an object are marked prior to the photographing stage, enabling the separation of surfaces in monochrome and low-texture objects. The effectiveness of the technique was demonstrated by comparing 3D models generated from both marked and unmarked objects against a CAD model based on actual object dimensions. Both 3D and 2D comparison analyses were conducted on plastic and metal objects.

The quantitative results revealed that the geometric accuracy of edges and corners improved significantly along the marked boundaries. Surfaces adjacent to these boundaries were also reconstructed with higher accuracy for both material types. Based on the analysis, it can be concluded that the boundary marking technique notably enhances the overall geometric accuracy of 3D models.

This technique presents a practical alternative to existing methods such as coating, masking, and other marking approaches commonly used in photogrammetric 3D reconstruction. It is cost-effective, easy to implement, and non-destructive, as the marks are temporary and can be removed without damaging the object. Future studies could explore the applicability of the proposed technique to a wider variety of object shapes with different geometric complexities and assess its effectiveness using alternative 3D scanning technologies. Additionally, the impact of variables such as marker color and contrast levels could be investigated to further evaluate the robustness and generalizability of the method in diverse real-world scenarios.

6 REFERENCES

[1] Helle, R. H. & Lemu, H. G. (2021). A case study on use of 3D scanning for reverse engineering and quality control. *Materials Today: Proceedings*, *45*(6), 5255-5262. https://doi.org/10.1016/j.matpr.2021.01.828

[2] Gessner, A., Ptaszyński, W., & Adam, W. (2022). Accuracy of the New Method of Alignment of Workpiece Using Structural-Light 3D Scanner. *Advances in Science and Technology Research Journal*, *16*(1), 1-14. https://doi.org/10.12913/22998624/144541

[3] Haleem, A., Javaid, M., Goyal, A., & Khanam, T. (2022). Redesign of car body by reverse engineering technique using steinbichler 3D scanner and projet 3D printer. *Journal of Industrial Integration and Management*, *7*(2), 171-182. https://doi.org/10.1142/S2424862220500074

[4] Simranjit Singh Sidhu, Sandeep Singh, & Onkar Singh Sidhu. (2025). Development of scaffolds using 3D printing for tissue engineering. *Journal of Management and Engineering Sciences*, *2*(1), 22-28. https://doi.org/10.61552/JMES.2025.01.002

[5] Lin, J.-R., Cao, J., Zhang, J.-P., van Treeck, C., & Frisch, J. (2019). Visualization of indoor thermal environment on mobile devices based on augmented reality and computational fluid dynamics. *Automation in Construction*, *103*, 26-40. https://doi.org/10.1016/j.autcon.2019.02.007

[6] Cansiz, E., Turan, F., & Arslan, Y. Z. (2016). Computer-Aided Design and Manufacturing of a Novel Maxillofacial Surgery Instrument: Application in the Sagittal Split Osteotomy. *Journal of Medical Devices*, *10*(4). https://doi.org/10.1115/1.4034297

[7] Mohamed, M. E., Bonello, P., Russhard, P., Procházka, P., Mekhalfia, M. L., & Tchuisseu, E. B. T. (2022). Experimental validation of FEM-computed stress to tip deflection ratios of aero-engine compressor blade vibration modes and quantification of associated uncertainties. *Mechanical Systems and Signal Processing*, *178*, 1-25. https://doi.org/10.1016/j.ymssp.2022.109257

[8] Tan, P. (2014*). Image-based modeling. InComputer Vision.* Boston, MA: Springer US.

[9] Costa, E. (2022). Survey and photogrammetry in underwater archaeological contexts at low visibility in the Venice lagoon. *Digital Applications in Archaeology and Cultural Heritage*, *24*, e00215. https://doi.org/10.1016/j.daach.2022.e00215

[10] Tsoraeva, E. N., Gadzhiev, R. K., Kuchiev, S. E., Pekh, A. A., & Mezhyan, S. A. (2021). Application of photogrammetric methods in architecture, construction and land management. *IOP Conference Series: Materials Science and Engineering*, *1083*(1), 012052. https://doi.org/10.1088/1757-899X/1083/1/012052

[11] Kingsland, K. (2020). Comparative analysis of digital photogrammetry software for cultural heritage. *Digital Applications in Archaeology and Cultural Heritage*, *18*, e00157. https://doi.org/10.1016/j.daach.2020.e00157

[12] Struck, R., Cordoni, S., Aliotta, S., Pérez-Pachón, L., & Gröning, F. (2019). *Application of photogrammetry in biomedical science. Biomedical Visualisation.* Switzerland: Springer Cham.

[13] Orun, A. B., Goodyer, E., & Smith, G. (2018). 3D non-invasive inspection of the skin lesions by close-range and low-cost photogrammetric techniques. *Image Analysis & Stereology*, *37*(1), 63. https://doi.org/10.5566/ias.1730

[14] Edelman, G. J. & Aalders, M. C. (2018). Photogrammetry using visible, infrared, hyperspectral and thermal imaging of crime scenes. *Forensic Science International*, *292*, 181-189. https://doi.org/10.1016/j.forsciint.2018.09.025

[15] Büyüksalih, G., Kan, T., Özkan, G. E., Meriç, M., Isın, L., & Kersten, T. P. (2020). Preserving the knowledge of the past through virtual visits: From 3D laser scanning to virtual reality visualisation at the Istanbul Çatalca İnceğiz caves. *PFG - Journal of Photogrammetry, Remote Sensing and Geoinformation Science*, *88*(2), 133-146. https://doi.org/10.1007/s41064-020-00091-3

[16] Bot, J. & Irschick, D. (2019). *Using 3D photogrammetry to create open-access models of live animals: 2D and 3D software solutions. 3D/VR in the Academic Library: Emerging Practices and Trends*. Arlington: Council on Library and Information Resources.

[17] Armesto, J., Lubowiecka, I., Ordóñez, C., & Rial, F. I. (2009). FEM modeling of structures based on close range digital photogrammetry. *Automation in Construction*, *18*(5), 559-569. https://doi.org/10.1016/j.autcon.2008.11.006

[18] Riveiro, B., Caamaño, J. C., Arias, P., & Sanz, E. (2011). Photogrammetric 3D modelling and mechanical analysis of masonry arches: An approach based on a discontinuous model of voussoirs. *Automation in Construction*, *20*(4), 380-388. https://doi.org/10.1016/j.autcon.2010.11.008

[19] Dixit, I., Kennedy, S., Piemontesi, J., Kennedy, B., & Krebs, C. (2019). *Which tool is test: 3D scanning or photogrammetry - It depends on the task. Biomedical Visualisation*. Switzerland: Springer Cham.

[20] Mohammadi, M., Rashidi, M., Mousavi, V., Karami, A., Yu, Y., & Samali, B. (2021). Quality evaluation of digital twins generated based on UAV photogrammetry and TLS: Bridge case study. *Remote Sensing*, *13*(17), 3499. https://doi.org/10.3390/rs13173499

[21] Ozendi, M., Akca, D., & Topan, H. (2023). A point cloud filtering method based on anisotropic error model. *The Photogrammetric Record*, *38*(184), 460-497. https://doi.org/10.1111/phor.12460

[22] Qingming, Z., Yubin, L., & Yinghui, X. (2009). Color-based segmentation of point clouds. *Laser scanning*, *38*(3), 155-161.

[23] Waltenberger, L., Rebay-Salisbury, K., & Mitteroecker, P. (2021a). Three-dimensional surface scanning methods in osteology: A topographical and geometric morphometric comparison. *American Journal of Physical Anthropology*, *174*(4), 846-858. https://doi.org/10.1002/ajpa.24204

[24] Chaiyasarn, K., Buatik, A., Mohamad, H., Zhou, M., Kongsilp, S., & Poovarodom, N. (2022). Integrated pixel-level CNN-FCN crack detection via photogrammetric 3D texture mapping of concrete structures. *Automation in Construction*, *140*, 104388. https://doi.org/10.1016/j.autcon.2022.104388

[25] Teo T, N., Marko, V., & Jarno, V. (2021). Open3DGen: open-source software for reconstructing textured 3D models from RGB-D images. *Proceedings of the 12th ACM Multimedia Systems Conference*. https://doi.org/10.1145/3458305

[26] Hernandez, A. & Lemaire, E. (2017). A smartphone photogrammetry method for digitizing prosthetic socket interiors. *Prosthetics & Orthotics International*, *41*(2), 210-214. https://doi.org/10.1177/0309364616664150

[27] Franke, J., Koutecký, T., Malý, M., Kalina, M., & Koutný, D. (2022). Study of process parameters of the atomizer-based spray gun for the application of a temporary matte coating for 3D scanning purposes. *Materials Chemistry and Physics*, *282*, 125950. https://doi.org/10.1016/j.matchemphys.2022.125950

[28] Nam, J., Valinasab, B., & Jun, B. G. (2017). Performance evaluation of atomization-based uniform spray coating for 3D scanning. *Journal of the Korean Society for Precision Engineering*, *34*(10), 689-693. https://doi.org/10.7736/KSPE.2017.34.10.689

[29] Valinasab, B., Rukosuyev, M., Lee, J., Ko, J., & Jun, M. B. G. (2015). Improvement of optical 3D scanner performance using atomization-based spray coating. *Journal of The Korean Society of Manufacturing Technology Engineers*, *24*(1), 23-30. https://doi.org/10.7735/ksmte.2015.24.1.023

[30] Murtiyoso, A. & Grussenmeyer, P. (2022). Automatic point cloud noise masking in close range photogrammetry for buildings using ai-based semantic labelling. *The International Archives of the Photogrammetry, Remote Sensing and Spatial Information Sciences*, *XLVI-2/W1-2022*, 389-393. https://doi.org/10.5194/isprs-archives-XLVI-2-W1-2022-389-2022

[31] Lerma, J. L., Navarro, S., Cabrelles, M., & Villaverde, V. (2010). Terrestrial laser scanning and close range photogrammetry for 3D archaeological documentation: the Upper Palaeolithic Cave of Parpalló as a case study. *Journal of Archaeological Science*, *37*(3), 499-507. https://doi.org/10.1016/j.jas.2009.10.011

[32] Medina, J. J., Maley, J. M., Sannapareddy, S., Medina, N. N., Gilman, C. M., & McCormack, J. E. (2020). A rapid and cost-effective pipeline for digitization of museum specimens with 3D photogrammetry. *PLOS ONE*, *15*(8), e0236417. https://doi.org/10.1371/journal.pone.0236417

[33] Fabio, R. & Sabry, E.-H. (2006). Image-based 3D modelling: A review. *The Photogrammetric Record*, *21*(115), 269-291. https://doi.org/10.1016/j.matchemphys.2022.125950

[34] Thomas, L., Stuart, R., Stephen, K., & Jan, B. (2019). Mathematical fundamentals. *Close-Range Photogrammetry and 3D Imaging*, 33-122. https://doi.org/10.1515/9783110607253-002

[35] Gessner, A., Staniek, R., & Bartkowiak, T. (2015). Computer-aided alignment of castings and machining optimization. *Part C: Journal of Mechanical Engineering Science*, *229*(3), 485-492. https://doi.org/10.1177/0954406214536380

[36] Guo, T., Capra, A., Troyer, M., Gruen, A., Brooks, A. J., Hench, J. L., Schmitt, R. J., Holbrook, S. J., & Dubbini, M. (2016). Accuracy assessment of underwater photogrammetric three dimensional modelling for coral reefs. *ISPRS - International Archives of the Photogrammetry, Remote Sensing and Spatial Information Sciences*, *XLI-B5*, 821-828. https://doi.org/10.5194/isprsarchives-XLI-B5-821-2016

[37] Ozimek, A., Ozimek, P., Skabek, K., & Łabędź, P. (2021). Digital Modelling and Accuracy Verification of a Complex Architectural Object Based on Photogrammetric Reconstruction. *Buildings*, *11*(5), 206. https://doi.org/10.3390/buildings11050206

[38] Silvester, C. M. & Hillson, S. (2020). A critical assessment of the potential for Structure-from-Motion photogrammetry to produce high fidelity 3D dental models. *American Journal of Physical Anthropology*, *173*(2), 381-392. https://doi.org/10.1002/ajpa.24109

[39] Tran, H., Khoshelham, K., & Kealy, A. (2019). Geometric comparison and quality evaluation of 3D models of indoor environments. *ISPRS Journal of Photogrammetry and Remote Sensing*, *149*, 29-39. https://doi.org/10.1016/ j.isprsjprs.2019.01.012

[40] Van Vlasselaer, N., Keelson, B., Scafoglieri, A., & Cattrysse, E. (2024). Exploring reliable photogrammetry techniques for 3D modeling in anatomical research and education. *Anatomical Sciences Education*, *17*(3), 674-682. https://doi.org/10.1002/ase.2391

[41] Milde, J., Dubnicka, M., & Buransky, I. (2023). Impact of powder coating types on dimensional accuracy in optical 3d scanning process. *MM Science Journal*, *2023*(4), 6800-6806. https://doi.org/10.17973/MMSJ.2023_11_2023084

[42] Pereira, J. R. M., de Lima e Silva Penz, I., & da Silva, F. P. (2019). Effects of different coating materials on three-dimensional optical scanning accuracy. *Advances in Mechanical Engineering*, *11*(4), 168781401984241. https://doi.org/10.1177/1687814019842416

[43] Remondino, F. & Menna, F. (2008). Image-based surface measurement for close-range heritage documentation. *ISPRS Journal of Photogrammetry and Remote Sensing*, *76*, 13-26.

[44] Luhmann, T., Robson, S., Kyle, S., & Boehm, J. (2023). *Close-range photogrammetry and 3D imaging*. Walter de Gruyter GmbH & Co KG.

[45] Cabero, I. & Epifanio, I. (2019). Archetypal analysis: An alternative to clustering for unsupervised texture segmentation. *Image Analysis & Stereology*, *38*(2), 151. https://doi.org/10.5566/ias.2052

[46] Fassi, F., Fregonese, L., Ackermann, S., & De Troia, V. (2013). Comparison between laser scanning and automated 3D modelling techniques to reconstruct complex and extensive cultural heritage areas. *ISPRS - International Archives of the Photogrammetry, Remote Sensing and Spatial Information Sciences*, *XL-5/W1*, 73-80.

Contact information:

Hasan Kemal SURMEN
Department of Automotive Technologies,
Istanbul University-Cerrahpasa,
Buyukcekmece, 34500, Istanbul, Türkiye
E-mail: hksurmen@iuc.edu.tr